

Fiber Bundle Networks: A Geometric Machine Learning Paradigm

Dong Liu

liudong@mit.edu

Abstract

We propose Fiber Bundle Networks (FiberNet), a novel machine learning framework integrating differential geometry with machine learning. Unlike traditional deep neural networks relying on black-box function fitting, we reformulate classification as interpretable geometric optimization on fiber bundles, where categories form the base space and wavelet-transformed features lie in the fibers above each category. We introduce two innovations: (1) learnable Riemannian metrics identifying important frequency feature components, (2) variational prototype optimization through energy function minimization. Classification is performed via Voronoi tessellation under the learned Riemannian metric, where each prototype defines a decision region and test samples are assigned to the nearest prototype, providing clear geometric interpretability. This work demonstrates that the integration of fiber bundle with machine learning provides interpretability and efficiency, which are difficult to obtain simultaneously in conventional deep learning.

Keywords: Fiber bundle, Riemannian metric, Variational Prototype Optimization, Energy functional, Wavelet transform, Voronoi Cell

1 Introduction

Consider the task of distinguishing the sound of ocean waves from the sound of a chair scraping against the floor. Ocean waves produce low-frequency periodic fluctuations (20-500 Hz) that evolve slowly over several seconds. Chair scraping produces high-frequency aperiodic noise (2000-8000 Hz) with sudden onsets. These two sounds have fundamental differences in their frequency characteristics. But how can an algorithm automatically learn that “low frequencies are more important for ocean waves” while “high frequencies are more important for scraping sounds”? How can we leverage the semantic knowledge that “ocean waves are similar to rain sounds but far from scraping sounds”?

Traditional deep learning implicitly learns these relationships through multi-layer structures [1], and while powerful, they provide little insight into what has been learned or

why it works [2, 3]. However, FiberNet explicitly models them through an interpretable geometric framework: a learnable Riemannian metric adaptively weights the importance of different frequency band features within categories, and a variational energy functional naturally injects semantic structure between categories.

FiberNet can be used for various tasks such as audio classification, image classification, text classification, gene sequence classification, etc. Correspondingly, different data types require appropriate feature extraction methods: audio can use wavelet transforms to capture time-frequency structure, images can use filters to extract multi-scale texture features, text can use word embeddings to capture semantic relationships, and gene sequences can use fragment frequency statistics to extract sequence patterns. We use audio classification as an example to introduce the classification mechanism of FiberNet.

The mainstream approach for audio classification is deep neural networks, such as learning feature representations of spectrograms through convolutional layers [4]. Despite the great success of deep learning, three key challenges remain: First, large-scale models have enormous parameter counts (ResNet-18 has approximately 11M parameters, PANNs has approximately 80M parameters [5]), making deployment on resource-constrained edge devices (such as smart speakers and hearing aids) challenging. Second, the models are black boxes, unable to explain why a certain sound is classified as “ocean waves” rather than “rain”, which is a major obstacle in critical applications such as medical acoustic diagnosis. Third, traditional cross-entropy loss functions ignore semantic relationships between categories—“ocean waves” and “rain” are both natural sounds and should be closer than “ocean waves” and “metal striking”, but cross-entropy treats all misclassifications equally.

We propose FiberNet, a geometric framework that makes these learning processes explicit through fiber bundles. The core idea is: modeling classification as a geometric optimization problem on fiber bundles. The category space is the base space, and all audio features corresponding to each category lie in the fiber space [6]. This modeling explicitly expresses the two-layer “category-feature” structure, allowing us to utilize geometric tools (sections, Riemannian metrics) and variational optimization methods within the fiber bundle framework.

FiberNet consists of three core components. First, a learnable diagonal Riemannian metric $G = \text{diag}(a_1, \dots, a_d)$, where weights $a_i > 0$ adaptively reflect the discriminability of each wavelet coefficient, reflecting the difference in the ability of different wavelet bases to capture category information. Traditional Euclidean distance treats all frequency bands equally [7], while in audio classification, the importance of different frequency bands varies significantly—for example, ocean wave sounds mainly rely on low-frequency components (50-500 Hz), while whistle sounds rely on high-frequency components (1000-4000 Hz). Metric learning allows the algorithm to automatically identify important frequency bands, reducing the influence of noise and irrelevant dimensions.

Second, variational optimization through energy minimization. Category prototypes serve as “representative” features for samples of that class, defined on the fiber bundle as the value of a section at the corresponding category, where the section is a mapping from category space to feature space. We optimize category prototypes by minimizing an energy functional. The energy includes three terms: attachment energy brings prototypes close to training samples of their category (e.g., fitting within the “ocean waves” class); tension energy encourages prototypes of semantically similar categories to be close (e.g., “ocean waves-rain”); repulsion energy ensures sufficient separation between different categories (e.g., “ocean waves-metal striking”).

Third, a classification strategy based on Voronoi partitioning. Finally, we train N category prototypes (N is the total number of categories). During classification prediction, we select the prototype with the smallest Riemannian distance. This process is equivalent to the feature space being naturally partitioned into N regions (N is the total number of categories) by the prototypes, and classification determines which Voronoi Cell centered on a prototype a new sample belongs to.

Our main contributions are as follows: (a) In theoretical innovation, we propose the novel machine learning paradigm of Fiber Bundle Networks, systematically applying fiber bundle theory from differential geometry to machine learning classification problems for the first time; (b) In interpretability, Riemannian metric weights reveal frequency band feature importance, and energy minimization yields prototype configurations encoding semantic relationships; (c) In algorithmic design, we propose a variational algorithm for jointly optimizing metrics and prototypes, and prove its convergence and geometric properties.

2 Related Work

Fiber bundles, as a core concept in differential geometry, have recently begun to be introduced into machine learning and data analysis, but related work is still relatively scarce. Courts and Kvinge (2021) [6] proposed Bundle Networks for exploring the fiber structure of many-to-one mappings. The core idea is to use local trivialization to decompose the space into the product of base space and fiber, thus naturally modeling the generative process—given output y , generate the set of inputs x satisfying $f(x) = y$ (i.e., the fiber). This work has a conceptual duality with the present paper: Bundle Networks focus on the generative problem (diversity from output to input), while FiberNet focuses on its inverse—the classification problem (mapping from input to output). Our section can be viewed as selecting a representative point for each category, while Bundle Networks focus on how to generate the entire fiber given a representative point. Both utilize the local structure of fiber bundles, but with complementary optimization objectives: they maximize generative diversity, we minimize classification uncertainty. The application of

geometric structures to machine learning has also been explored in other contexts, such as Riemannian geometry for deep learning architectures [8] and manifold learning [9]. Scoccola and Perea (2022)’s [10] FibeRed algorithm uses vector bundles for dimensionality reduction from the perspective of topological data analysis, modeling data as vector bundles so that the base space captures large-scale topology while fibers capture local geometry. This work shares with the present paper the use of fiber bundle hierarchical structure to model complex data—the base space carries global information, fibers carry local details. The difference is that FibeRed’s base space is the topological structure of the data (discovered through topological inference), while FiberNet’s base space is the category space, achieving classification by learning sections (mapping from categories to features) and metrics (geometry of feature space).

3 FiberNet Mathematical Framework

3.1 Fiber Bundle Structure

We use the audio classification problem as an example to model the Fiber Bundle Network algorithm. A fiber bundle is a geometric structure that naturally accommodates the representation of categories, features, and their relationships. Let N be the total number of categories, the category set be $C = \{c_1, c_2, \dots, c_N\}$, and the feature vector dimension be d .

Definition 3.1 (Classification Fiber Bundle). *The fiber bundle for an N -class classification problem is a triple (\mathcal{E}, C, π) , where:*

- *Base space: category set C*
- *Fiber $F_c = \{c\} \times \mathbb{R}^d$: all “category-feature” pairs for category c , where the second component $v \in \mathbb{R}^d$ is a d -dimensional feature vector*
- *Total space $\mathcal{E} = C \times \mathbb{R}^d$: the set of all “category-feature” pairs*
- *Projection map $\pi : \mathcal{E} \rightarrow C$, $\pi(c, v) = c$ (extracting the category label)*

This constitutes a trivial fiber bundle (\mathcal{E}, C, π) . A trivial bundle means that the feature space structure is the same for all categories, all isomorphic to \mathbb{R}^d , allowing features of different categories to be compared within a unified framework. For example, features of “ocean waves” and features of “metal striking”, although belonging to different fibers, can both compute distances under the same Riemannian metric.

For better geometric intuition, we can imagine the category space C as a line segment or plane, with a d -dimensional fiber “column” “erected” above each category $c \in C$. The total space \mathcal{E} is the union of all these columns. An audio sample (c, v) corresponds to a point on one of these columns.

3.2 Wavelet Feature Extraction

Audio signals are essentially non-stationary signals—their frequency characteristics evolve over time. Understanding audio requires not only knowing “what frequencies appear” but also “when they appear”. The Fourier transform only provides global frequency information, completely losing time localization capability. The Short-Time Fourier Transform (STFT) introduces time-frequency analysis but is limited by fixed windows, unable to simultaneously achieve precise time and frequency localization. The wavelet transform solves this dilemma through multi-scale adaptive analysis: low-frequency components use long time windows to capture periodic structures, high-frequency components use short windows to locate transient events. This makes wavelet transform a natural choice for audio feature representation [11, 12].

Discrete Wavelet Transform

Given an audio signal $s(t)$ with sampling rate f_s . According to the Nyquist theorem, the frequency range contained in the signal is $[0, f_s/2]$. The core idea of the Discrete Wavelet Transform (DWT) is: repeatedly split the low-frequency part of the signal in half, extracting frequency components layer by layer.

Layer 1 decomposition. Starting from the original signal S , we use a pair of filters (low-pass filter and high-pass filter) to split the signal into two parts:

$$A_1 : \text{Approximation coefficients (low-frequency part), frequency range } [0, f_s/4], \quad (1)$$

$$D_1 : \text{Detail coefficients (high-frequency part), frequency range } [f_s/4, f_s/2]. \quad (2)$$

D_1 captures the fastest changes in the signal, such as high-frequency noise. A_1 preserves relatively slow changes but still contains mid-low frequency information and needs further decomposition.

Layer 2 decomposition. Next, we retain D_1 (no further processing) and continue decomposing A_1 . We treat A_1 as a new “signal” and decompose it again using low-pass/high-pass filters:

$$A_1 \rightarrow \begin{cases} A_2 : \text{Lower frequency part, frequency range } [0, f_s/8] \\ D_2 : \text{Mid frequency part, frequency range } [f_s/8, f_s/4]. \end{cases} \quad (3)$$

Note the change in frequency range. Original signal $[0, f_s/2]$. After layer 1 decomposition, A_1 only contains $[0, f_s/4]$ (frequency range halved). After layer 2 decomposition, A_2 only contains $[0, f_s/8]$ (frequency range halved again).

Repeat to layer L decomposition. Continue this process: each time decompose the current approximation coefficients $A_{\ell-1}$ to obtain new A_ℓ and D_ℓ . The recursive

formula is:

$$A_{\ell-1} \rightarrow \begin{cases} A_{\ell} : \text{frequency range } [0, f_s/2^{\ell+1}] \\ D_{\ell} : \text{frequency range } [f_s/2^{\ell+1}, f_s/2^{\ell}]. \end{cases} \quad (4)$$

After L layers of decomposition, the original signal is completely decomposed as:

$$S = A_L + D_L + D_{L-1} + \cdots + D_2 + D_1 = A_L + \sum_{\ell=1}^L D_{\ell}. \quad (5)$$

The entire wavelet decomposition process forms a binary tree, with each node representing a frequency band (see Figure 1):

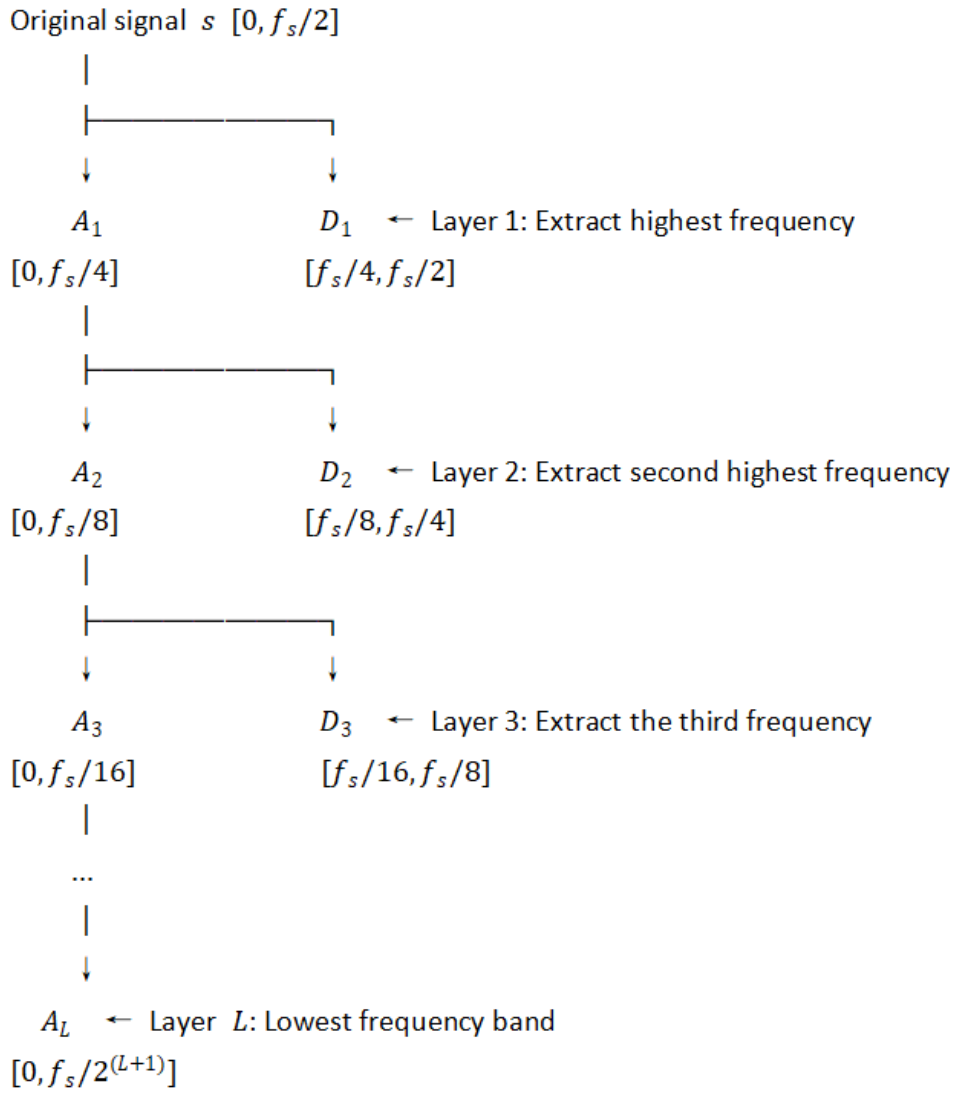


Figure 1: Wavelet decomposition binary tree structure. Each decomposition layer halves the frequency range, extracting frequency components from high to low. The leaf nodes $\{D_1, D_2, \dots, D_L, A_L\}$ form the final $L + 1$ frequency bands.

Therefore, we can see that with each layer of wavelet transform decomposition, the

frequency range halves ($[0, f_s/2^\ell] \rightarrow [0, f_s/2^{\ell+1}]$). The “leaf nodes” of the tree are the final retained frequency components $\{D_1, D_2, \dots, D_L, A_L\}$, a total of $L + 1$ frequency bands, arranged from high to low.

The essence of wavelet transform multi-resolution analysis. This layer-by-layer decomposition achieves adaptive time-frequency trade-off, thus possessing two advantages that the Short-Time Fourier Transform cannot simultaneously have. (a) Precise time localization: High-frequency components (such as D_1, D_2) correspond to short time windows, allowing precise time localization, thus suitable for capturing transient events (such as strikes, explosions); (b) Precise frequency resolution: Low-frequency components correspond to long windows, covering narrow frequency bands (e.g., A_L only covers $[0, f_s/2^{L+1}]$, with bandwidth much narrower than $[f_s/4, f_s/2]$ covered by D_1), enabling precise distinction of nearby frequencies, suitable for capturing periodic structures (such as ocean wave sounds, engine sounds). Therefore, this adaptive long-short window mechanism allows wavelet transform to balance precise localization in both time and frequency, which is exactly what the Short-Time Fourier Transform’s fixed window cannot achieve.

Orthogonal wavelet basis. We choose orthogonal wavelet bases (such as Daubechies wavelets [13]) for decomposition, which are implemented through a pair of orthogonal low-pass/high-pass filters, ensuring orthogonality between frequency bands:

$$\langle D_i, D_j \rangle = 0 \quad (i \neq j), \quad \langle A_L, D_i \rangle = 0 \quad \forall i. \quad (6)$$

This property is crucial, meaning that information in different frequency bands is approximately decoupled, providing a theoretical basis for subsequent diagonal Riemannian metric learning. Due to orthogonality between frequency bands, we can independently assign weights a_i to each frequency band (reflecting its importance for classification) without considering complex coupling between frequency bands—otherwise, a full metric matrix would be needed, requiring $O(d^2)$ parameters; whereas a diagonal metric only needs d parameters, significantly reducing the number of training parameters.

Energy conservation. By Parseval’s theorem, the total energy of the signal is preserved in the wavelet domain:

$$\|S\|^2 = \|A_L\|^2 + \sum_{\ell=1}^L \|D_\ell\|^2. \quad (7)$$

The energy distribution $\frac{\|A_L\|^2}{\|S\|^2}, \frac{\|D_L\|^2}{\|S\|^2}, \dots, \frac{\|D_1\|^2}{\|S\|^2}$ is the frequency characteristic fingerprint of sound categories.

Feature vector construction. Utilizing the sparsity of audio signals in the wavelet domain (energy concentrated in a few coefficients, most coefficients close to zero), we retain the top k largest energy coefficients from each frequency band, capturing the main

energy distribution characteristics of that frequency segment. Concatenating yields a fixed-dimension feature vector:

$$v = [A_L^{(1:k)}, D_L^{(1:k)}, \dots, D_1^{(1:k)}] \in \mathbb{R}^d, \quad d = (L + 1) \cdot k. \quad (8)$$

The key requirement here is consistency, i.e., all audio uses the same wavelet basis, decomposition layers, and coefficient retention strategy, ensuring that each dimension of the feature vector v has the same physical meaning. For example, the first k dimensions of each sample’s feature vector always correspond to the main energy components of the lowest frequency band, facilitating cross-sample comparison.

Role of wavelet transform in fiber bundles. The wavelet transform defines a mapping from time-domain signal space to feature space:

$$\Phi : s(t) \mapsto v \in \mathbb{R}^d. \quad (9)$$

In the fiber bundle framework (Section 3.1), labeled training samples (c, s) are mapped to points in the total space \mathcal{E} :

$$(c, s) \mapsto (c, \Phi(s)) = (c, v) \in \mathcal{E} = C \times \mathbb{R}^d. \quad (10)$$

Since audio of the same class has similar physical production mechanisms, their frequency energy distribution patterns are also similar. For example, ocean wave sounds all come from periodic motion and collision of water bodies, with energy concentrated in low-frequency bands; metal strikes are all solid transient collisions, with energy distributed in high-frequency bands. This physical similarity is reflected in the wavelet domain as: wavelet coefficient energy distributions between same-class audio are more similar than different-class audio, and extracted feature vectors are closer. Additionally, orthogonality between subbands allows the diagonal Riemannian metric (Section 3.3) to independently adjust the contribution of each frequency band.

The training set is finally represented as $\mathcal{D} = \{(c_1, v_1), \dots, (c_M, v_M)\}$, where $v_i \in \mathbb{R}^d$ is a wavelet feature vector and $c_i \in C$ is a category label. The next section will define a learnable Riemannian metric on this feature space.

3.3 Riemannian Metric

We define a diagonal Riemannian metric in the fiber direction (feature space \mathbb{R}^d) of the fiber bundle, represented by the metric tensor $G = \text{diag}(a_1, \dots, a_d)$, where $a_i > 0$ is the weight for the i -th feature dimension (corresponding to a coefficient of some frequency

band). The Riemannian distance between two feature vectors $v_1, v_2 \in \mathbb{R}^d$ is:

$$d_G(v_1, v_2) = \sqrt{\sum_{i=1}^d a_i (v_{1,i} - v_{2,i})^2} \quad (11)$$

This formulation is related to Mahalanobis distance [14] but with learnable diagonal structure.

The diagonal form has advantages in three aspects: parameter efficiency, interpretability, and theoretical foundation. First, it only requires d parameters, far fewer than the $d(d+1)/2$ parameters of a full metric tensor (when $d = 250$, reduced from 31,375 to 250). Second, each weight a_i directly corresponds to the importance of a frequency band coefficient, i.e., large a_i means that dimension contributes significantly to classification. Third, orthogonality between wavelet subbands ensures independence of feature dimensions, and the diagonal metric is sufficient to capture the main geometric structure.

To ensure positive definiteness of the metric ($a_i > 0$), we adopt exponential reparameterization $a_i = \exp(\theta_i)$, where $\theta_i \in \mathbb{R}^d$ is an unconstrained real parameter. During optimization, we perform gradient descent directly on θ , automatically satisfying the positive definiteness constraint. Initialization $\theta = 0$ corresponds to Euclidean metric ($a_i = 1$).

3.4 Sections and Prototypes

The section is a core concept in fiber bundle geometry, providing a mathematical framework for systematically selecting representative points in the fiber of each category.

Definition 3.2 (Section). *A section is a map $s : C \rightarrow \mathcal{E}$ satisfying the composition condition $\pi \circ s = id_C$, i.e., for each category $c \in C$, the value of the section at c , denoted $s(c)$, must belong to the corresponding fiber $F_c = \{c\} \times \mathbb{R}^d$.*

Since the total space $\mathcal{E} = C \times \mathbb{R}^d$ is the direct product of category space and feature space, the value of the section can be written as $s(c) = (c, v_c)$, where $v_c \in \mathbb{R}^d$. To simplify notation, we equivalently represent the section as a map $s : C \rightarrow \mathbb{R}^d$, where $s(c) = v_c$ is the prototype feature vector for category c .

Geometrically, one can imagine a set of vertical fiber “columns” stacked above the category space, with the section selecting a representative point (prototype) on each column. The configuration formed by these prototypes should reflect the semantic relationships of categories: prototypes of semantically similar categories (such as “ocean waves” and “rain”) should be close, and prototypes of semantically different categories (such as “ocean waves” and “metal striking”) should be distant. A good section is “smooth”, not jumping dramatically between semantically similar categories.

The section is determined by N d -dimensional vectors $\{s(c_1), \dots, s(c_N)\}$, totaling $N \times d$ parameters. Each prototype is initialized as the mean of training samples of that category:

$$s(c) = \frac{1}{|D_c|} \sum_{v_i: c_i=c} v_i. \quad (12)$$

For example, for a dataset with 50 classes and dimension 250, the section is 50 vectors of 250 dimensions, each vector representing the corresponding category. A good section should satisfy: $d_G(s(\text{“sea waves”}), s(\text{“rain”}))$ is small, while $d_G(s(\text{“sea waves”}), s(\text{“metal striking”}))$ is large. This geometric configuration conforming to semantic intuition will be automatically achieved through energy functional optimization in the next section.

3.5 Variational Energy Functional

The section is optimized by minimizing an energy functional. The energy design is based on variational principles [15], balancing three objectives:

$$E[s] = E_{\text{attachment}}[s] + \lambda_1 E_{\text{tension}}[s] + \lambda_2 E_{\text{repulsion}}[s]. \quad (13)$$

The first term is the attachment energy, defined as:

$$E_{\text{attachment}}[s] = \frac{1}{M} \sum_{i=1}^M d_G^2(v_i, s(c_i)). \quad (14)$$

It ensures that each prototype is close to the training samples of its category. One can imagine training samples connected to the corresponding prototype through “springs”, with the attachment energy being the sum of all spring potential energies, where the spring stiffness coefficient is determined by the metric G . Taking the “ocean waves” category as an example, all ocean wave sound samples $\{v_i : c_i = \text{sea waves}\}$ “pull” the prototype $s(\text{sea waves})$ toward their average position, and the metric G ’s weights $\{a_i\}$ determine the relative strength of different frequency bands in this “pulling force”.

The second term is the tension energy, defined as:

$$E_{\text{tension}}[s] = \sum_{(c_i, c_j) \in \mathcal{E}_{\text{sem}}} w_{ij} d_G^2(s(c_i), s(c_j)). \quad (15)$$

It encourages prototypes of semantically similar categories to be close. Here \mathcal{E}_{sem} is the adjacency relation set, and w_{ij} are edge weights. Adjacency relations are determined through semantic similarity of category names: first, use a word embedding model [16] to convert each category name to a vector emb_c , then calculate cosine similarity between

any two categories:

$$\text{sim}(c_i, c_j) = \frac{\text{emb}_{c_i}^T \text{emb}_{c_j}}{\|\text{emb}_{c_i}\| \|\text{emb}_{c_j}\|}. \quad (16)$$

For each category, we select the K categories with highest similarity (typically K is 2 or 3) as neighbors, forming the adjacency graph \mathcal{E}_{sem} . Edge weights are obtained through normalized similarity:

$$w_{ij} = \frac{\text{sim}(c_i, c_j)}{\sum_{c_k \in N(c_i)} \text{sim}(c_i, c_k)}. \quad (17)$$

where $N(c_i)$ is the neighbor set of c_i . For example, neighbors of “chair creaking” are “door_creak” (weight 0.5), “wood creak” (weight 0.3), “floor creak” (weight 0.2), all household creaking sounds.

The tension energy has a clear geometric-physical interpretation. From a physical perspective, prototypes are like mass points on a spring network, with semantically similar prototypes (such as “rain-stream sound”) connected by strong springs (large w_{ij}), and minimizing total potential energy brings similar prototypes together. From a geometric perspective, tension energy corresponds to discrete Dirichlet energy [17], encouraging smooth variation of the section between semantically similar categories, which is consistent with classical principles in variational calculus, where the energy minimization process makes the solution tend toward smoothness.

The third term is the repulsion energy, defined as:

$$E_{\text{repulsion}}[s] = \sum_{i \neq j} \max(0, \text{margin} - d_G(s(c_i), s(c_j)))^2. \quad (18)$$

It penalizes prototypes that are too close (less than margin), like repulsive force between charged particles, ensuring different categories maintain separation in feature space.

The three energy terms form a balance: attachment energy is an “internal force”, acting within the same category, bringing prototypes close to same-class samples; tension energy is an “external local force”, only acting on semantically adjacent categories, pulling similar prototypes together; repulsion energy is an “external global force”, acting on all category prototype pairs, pushing them apart. Even if “ocean waves” and “rain” are semantically similar, repulsion energy still ensures they maintain at least margin distance, avoiding classification confusion.

Hyperparameters λ_1 and λ_2 control this balance: large λ_1 makes the section smoother (semantic clustering more evident); large λ_2 makes decision boundaries wider (category separation clearer).

Energy Minimization. The optimal section s^* is obtained by minimizing the energy functional:

$$s^* = \arg \min_s E[s]. \quad (19)$$

With fixed metric G , s^* satisfies the variational condition:

$$\frac{\delta E}{\delta s} = 0. \quad (20)$$

In the discrete case, this is equivalent to: for each category $c \in C$,

$$\frac{\partial E}{\partial s(c)} = 0. \quad (21)$$

This corresponds to a stable equilibrium state in mechanics: attachment force (pulling prototypes toward samples), tension (pulling semantically similar prototypes together), and repulsion force (pushing all prototypes apart) reach dynamic balance.

3.6 Unified Optimization Framework for Energy Minimization

We jointly optimize the section s and metric G through a unified energy functional:

$$\min_{s,G} E[s, G(\theta)] = \min_{s,G} E_{\text{attachment}}[s, G] + \lambda_1 E_{\text{tension}}[s, G] + \lambda_2 E_{\text{repulsion}}[s, G], \quad (22)$$

where $s = (s(c_1), \dots, s(c_N))$ is the prototype configuration, $\theta = (\theta_1, \dots, \theta_d) \in \mathbb{R}^d$ is the metric parameter, and $G = \text{diag}(\exp(\theta_1), \dots, \exp(\theta_d))$.

Metric weights are automatically learned through energy minimization, without requiring additional loss functions. The three components of the energy functional embody the key mechanisms of metric learning: attachment energy automatically reduces weights of dimensions with large intra-class variance and increases weights of dimensions with high intra-class consistency by minimizing weighted intra-class distance; tension energy further encourages semantically similar categories to be close on key dimensions, reinforcing semantic structure; repulsion energy increases weights of dimensions that can effectively distinguish different categories, ensuring clear classification boundaries. The three work synergistically to automatically discover frequency band combinations most useful for classification.

The optimal solution (s^*, G^*) satisfies the variational condition:

$$\frac{\partial E}{\partial s(c)} = 0, \quad \forall c \in C; \quad \frac{\partial E}{\partial \theta_i} = 0, \quad \forall i = 1, \dots, d. \quad (23)$$

From a physical perspective, this corresponds to a stable equilibrium state of the system: for the prototype configuration, attachment force, tension, and repulsion force reach dynamic balance at each prototype; for metric weights, the importance of different frequency bands reaches optimal allocation, minimizing total energy.

The core advantage of this unified framework is: metrics and prototypes are jointly optimized through the same objective, mutually adapting. The metric shapes the geo-

metric structure of the feature space, guiding the configuration of prototypes; conversely, the distribution of prototypes influences metric learning. This avoids the complexity of multi-objective trade-offs in traditional metric learning methods while providing clear geometric interpretation.

4 Algorithm Design

This section introduces the algorithm for solving the optimization problem in Section 3. We adopt an alternating optimization strategy: fix metric G to optimize section s , then fix section s to optimize metric parameter θ , iterating until convergence [18]. Convergence analysis of alternating optimization is in Appendix A.

4.1 Alternating Optimization

The main loop of the algorithm contains two alternating steps. In the t -th iteration, we first fix metric $G^{(t)}$ and update section $s^{(t+1)}$ through gradient descent to reduce energy $E[s, G^{(t)}]$; then fix section $s^{(t+1)}$ and update metric parameter $\theta^{(t+1)}$ through gradient descent to reduce energy $E[s^{(t+1)}, G(\theta)]$.

Initialization is crucial for convergence speed and solution quality. We initialize each prototype as the mean of training samples of the corresponding category: $s^{(0)}(c) = \frac{1}{|D_c|} \sum_{v_i \in D_c} v_i$, providing a reasonable starting point. Metric parameters are initialized as $\theta^{(0)} = 0$, corresponding to Euclidean metric ($a_i = 1$), starting optimization from fair geometry and gradually discovering important frequency bands.

4.2 Convergence Criteria

The algorithm terminates when any of the following conditions is met: maximum number of iterations T_{\max} is reached (e.g., 100 iterations); energy change is less than threshold ϵ (e.g., $|E^{(t+1)} - E^{(t)}| < 10^{-4}$).

4.3 Classification Inference

After training is complete, we obtain the optimal prototype configuration $s^* = \{s^*(c_1), \dots, s^*(c_N)\}$ and optimal metric G^* . For a new test sample, first extract wavelet features $v_{\text{test}} = \Phi(s_{\text{test}})$, then calculate its Riemannian distance to all prototypes $d_{G^*}(v_{\text{test}}, s^*(c_i))$, and predict the category as the nearest prototype:

$$\hat{c} = \arg \min_{c \in C} d_{G^*}(v_{\text{test}}, s^*(c)). \quad (24)$$

This is a prototype-based nearest neighbor classifier [19], but both the metric and prototypes have undergone geometric optimization. From a geometric perspective, this corresponds to Voronoi partitioning of the feature space under Riemannian metric G^* , with each prototype defining a Voronoi cell (decision region) [20].

4.4 Algorithm Pseudocode

For ease of understanding and implementation, Algorithm 1 provides complete pseudocode for FiberNet, including preprocessing, alternating optimization, and inference stages.

Algorithm 1 FiberNet: Classification via Fiber Bundle

Require: Training set $\mathcal{D} = \{(c_i, s_i)\}_{i=1}^M$, hyperparameters λ_1, λ_2, K , margin

Ensure: Optimal prototypes s^* , optimal metric G^* , class prediction \hat{c}

- 1: Extract wavelet features: $v_i \leftarrow \Phi(s_i), \forall i$
 - 2: Build adjacency graph \mathcal{E} from class name embeddings (top- K neighbors)
 - 3: Initialize: $s^{(0)}(c) \leftarrow$ class mean, $\theta^{(0)} \leftarrow \mathbf{0}$, $G^{(0)} \leftarrow I$
 - 4: **for** $t = 0$ to $T_{\max} - 1$ **do**
 - 5: Fix $G^{(t)}$, update $s^{(t+1)}$ by gradient descent on $E[s, G^{(t)}]$
 - 6: where $E = E_{\text{att}} + \lambda_1 E_{\text{ten}} + \lambda_2 E_{\text{rep}}$
 - 7: Fix $s^{(t+1)}$, update $\theta^{(t+1)}$ by gradient descent on $E[s^{(t+1)}, G(\theta)]$
 - 8: $G^{(t+1)} \leftarrow \text{diag}(\exp(\theta^{(t+1)}))$
 - 9: **if** $|E^{(t+1)} - E^{(t)}| < \epsilon$ **then**
 - 10: **break**
 - 11: **end if**
 - 12: **end for**
 - 13: **return** $s^* \leftarrow s^{(T)}$, $G^* \leftarrow G^{(T)}$
 - 14: **Inference:** For test sample s_{test} , predict $\hat{c} \leftarrow \arg \min_c d_{G^*}(\Phi(s_{\text{test}}), s^*(c))$
-

5 Discussion

This paper proposes FiberNet, an audio classification framework based on fiber bundle geometry. Our core contribution is reformulating the classification problem as variational optimization on fiber bundles: section $s : C \rightarrow \mathbb{R}^d$ maps category space to feature space, Riemannian metric G defines the geometric structure of feature space, and a unified energy functional $E[s, G]$ optimizes both simultaneously. The key insight of this geometric perspective is that metrics and prototypes should be learned collaboratively—traditional methods seek prototypes in fixed Euclidean space, while we allow the space itself to “bend” to fit the data. Attachment energy, tension energy, and repulsion energy

correspond to data fitting, semantic smoothness, and category separation respectively, unified naturally through variational principles without manually balancing multiple loss functions. We prove convergence of the alternating optimization algorithm: the energy sequence monotonically decreases and converges. This convergence guarantee is based on good mathematical properties of the energy—attachment and tension energies are convex or log-convex with respect to subproblems, repulsion energy is non-convex but bounded, and overall energy is non-negative and lower bounded. From a broader perspective, FiberNet, inspired by fiber bundles and using energy functional minimization as a tool, establishes a new machine learning paradigm, providing new perspectives and tools for classification problems.

References

- [1] Y. LeCun, Y. Bengio, and G. Hinton. Deep learning. *Nature*, 521(7553):436–444, 2015.
- [2] Y. Zhang, P. Tiño, A. Leonardis, and K. Tang. A survey on neural network interpretability. *IEEE Transactions on Emerging Topics in Computational Intelligence*, 5(5):726–742, 2021.
- [3] Z. C. Lipton. The mythos of model interpretability: In machine learning, the concept of interpretability is both important and slippery. *Queue*, 16(3):31–57, 2018.
- [4] S. Abdoli, P. Cardinal, and A. L. Koerich. End-to-end environmental sound classification using a 1d convolutional neural network. *Expert Systems with Applications*, 136:252–263, 2019.
- [5] Q. Kong, Y. Cao, T. Iqbal, Y. Wang, W. Wang, and M. D. Plumbley. Panns: Large-scale pretrained audio neural networks for audio pattern recognition. In *IEEE/ACM Transactions on Audio, Speech, and Language Processing*, volume 28, pages 2880–2894, 2020.
- [6] N. Courts and H. Kvinge. Bundle networks: Fiber bundles, local trivializations, and a generative approach to exploring many-to-one maps. arXiv preprint arXiv:2110.06983, 2021.
- [7] C. Scarvelis and J. Solomon. Riemannian metric learning via optimal transport. In *International Conference on Learning Representations*. OpenReview, May 2023.
- [8] X. Pennec, P. Fillard, and N. Ayache. A riemannian framework for tensor computing. *International Journal of Computer Vision*, 66(1):41–66, 2006.

- [9] J. B. Tenenbaum, V. Silva, and J. C. Langford. A global geometric framework for nonlinear dimensionality reduction. *Science*, 290(5500):2319–2323, 2000.
- [10] L. Scoccola and J. A. Perea. Fibered: Fiberwise dimensionality reduction of topologically complex data with vector bundles. arXiv preprint arXiv:2206.06513, 2022.
- [11] S. Waldekar and G. Saha. Analysis and classification of acoustic scenes with wavelet transform-based mel-scaled features. *Multimedia Tools and Applications*, 79(11):7911–7926, 2020.
- [12] S. G. Mallat. A theory for multiresolution signal decomposition: the wavelet representation. *IEEE Transactions on Pattern Analysis and Machine Intelligence*, 11(7):674–693, 1989.
- [13] I. Daubechies. *Ten lectures on wavelets*. SIAM, 1992.
- [14] P. C. Mahalanobis. On the generalized distance in statistics. *Proceedings of the National Institute of Sciences of India*, 2(1):49–55, 1936.
- [15] R. Courant and D. Hilbert. *Methods of mathematical physics, volume I*. John Wiley & Sons, 1989.
- [16] T. Mikolov, K. Chen, G. Corrado, and J. Dean. Efficient estimation of word representations in vector space. *arXiv preprint arXiv:1301.3781*, 2013.
- [17] U. Pinkall and K. Polthier. Computing discrete minimal surfaces and their conjugates. *Experimental Mathematics*, 2(1):15–36, 1993.
- [18] J. C. Bezdek and R. J. Hathaway. Convergence of alternating optimization. *Neural, Parallel & Scientific Computations*, 11(4):351–368, 2003.
- [19] T. Cover and P. Hart. Nearest neighbor pattern classification. *IEEE Transactions on Information Theory*, 13(1):21–27, 1967.
- [20] F. Aurenhammer, R. Klein, and D. T. Lee. *Voronoi diagrams and Delaunay triangulations*. World Scientific Publishing Company, 2013.
- [21] W. Rudin. *Principles of mathematical analysis*. McGraw-Hill, 3rd edition, 1976.

A Convergence Proof for Alternating Optimization

Lemma A.1 (Energy Monotone Decrease). *The energy sequence $\{E^{(t)}\}_{t=0}^{\infty}$ generated by the alternating optimization algorithm satisfies:*

$$E^{(t+1)} \leq E^{(t)}, \quad \forall t \geq 0. \quad (25)$$

Proof. In the t -th iteration:

Fix $G^{(t)}$, minimize $E[s, G^{(t)}]$ through gradient descent to obtain $s^{(t+1)}$:

$$E[s^{(t+1)}, G^{(t)}] \leq E[s^{(t)}, G^{(t)}]. \quad (26)$$

Fix $s^{(t+1)}$, minimize $E[s^{(t+1)}, G]$ through gradient descent to obtain $G^{(t+1)}$:

$$E[s^{(t+1)}, G^{(t+1)}] \leq E[s^{(t+1)}, G^{(t)}]. \quad (27)$$

Combining the two steps:

$$E^{(t+1)} = E[s^{(t+1)}, G^{(t+1)}] \leq E[s^{(t+1)}, G^{(t)}] \leq E[s^{(t)}, G^{(t)}] = E^{(t)}. \quad (28)$$

Therefore the energy sequence monotonically decreases. \square

Lemma A.2 (Energy Lower Bound). *The energy functional satisfies $E[s, G] \geq 0$ for all (s, G) .*

Proof. The energy functional consists of three terms:

(1) Attachment energy:

$$E_{\text{att}} = \frac{1}{M} \sum_{i=1}^M d_G^2(v_i, s(c_i)) = \frac{1}{M} \sum_{i=1}^M \sum_{j=1}^d a_j (v_{i,j} - s(c_i)_j)^2 \geq 0, \quad (29)$$

because $a_j = \exp(\theta_j) > 0$ and squared terms are non-negative.

(2) Tension energy:

$$E_{\text{ten}} = \sum_{(i,j) \in \mathcal{E}} w_{ij} d_G^2(s(c_i), s(c_j)) \geq 0, \quad (30)$$

because $w_{ij} \geq 0$ (normalized similarity) and distance squared is non-negative.

(3) Repulsion energy:

$$E_{\text{rep}} = \sum_{i \neq j} \max(0, \text{margin} - d_G(s(c_i), s(c_j)))^2 \geq 0, \quad (31)$$

because $\max(0, \cdot)^2 \geq 0$.

Therefore:

$$E = E_{\text{att}} + \lambda_1 E_{\text{ten}} + \lambda_2 E_{\text{rep}} \geq 0. \quad (32)$$

\square

Theorem A.1 (Energy Sequence Convergence). *The energy sequence $\{E^{(t)}\}$ generated*

by the alternating optimization algorithm converges, i.e., there exists $E^* \geq 0$ such that:

$$\lim_{t \rightarrow \infty} E^{(t)} = E^*. \quad (33)$$

Proof. By Lemma A.1, $\{E^{(t)}\}$ is monotonically decreasing. By Lemma A.2, $E^{(t)} \geq 0$ for all t .

According to the Monotone Convergence Theorem [21]: a monotonically decreasing sequence with a lower bound must converge.

Therefore $\lim_{t \rightarrow \infty} E^{(t)} = E^*$ exists and $E^* \geq 0$. \square